DOI: https://doi.org/10.26565/2304-6201-2025-68-04

UDC 517.9:519.6

Koshkin Andrii *assistant of the Department of Applied Mathematics*
Kharkiv National University of Radio Electronics, Nauky Ave. 14, Kharkiv, Ukraine, 61166
e-mail: andrii.koshkin@nure.ua;
https://orcid.org/0009-0005-0970-0403

Strelnikova Olena *Professor, Doctor of Science (Engineering)*
Kharkiv National University of Radio Electronics, Nauky Ave. 14, Kharkiv, Ukraine, 61166
leading researcher
Anatolii Pidhornyi Institute of Power Machines and Systems of NAS of Ukraine, Komunalnykiv street 2/10, Kharkiv, Ukraine, 61046
e-mail: olena.strelnikova@nure.ua;
https://orcid.org/0000-0003-0707-7214

Bending analysis of multiply-connected anisotropic plates with elastic inclusions

Relevance. Determining the stress-strain state of thin anisotropic plates with foreign elastic inclusions under transverse bending is an important engineering problem. However, the general case of a plate with multiple, arbitrarily arranged inclusions has lacked an effective numerical or analytical solution due to significant mathematical and computational difficulties.
Objective. The purpose of this work is to develop a new approximate method for determining the stress state of a thin anisotropic plate containing a group of arbitrarily located elliptical or linear elastic inclusions.
Methods. The method is based on the application of S. G. Lekhnitskii's complex potentials. The problem is reduced to determining functions of generalized complex variables for the plate-matrix and the inclusions. These potentials are represented by corresponding Laurent series and Faber polynomials. The generalized least squares method (GLSM) is used to satisfy the contact boundary conditions on the inclusion contours. This reduces the problem to an overdetermined system of linear algebraic equations, which is solved using singular value decomposition (SVD).
Results. The developed method was validated by comparison with the known exact analytical solution for a plate with a single elliptical inclusion, showing perfect agreement. Numerical studies were conducted to analyze the influence of the relative stiffness of the inclusions, the distances between them, and their geometric characteristics on the bending moment values. It was established that the interaction between inclusions is significant and leads to a substantial increase in moments at small distances. Isotropic plates are considered as a special case of anisotropic ones.
Conclusions. It was established for the first time that for linear elastic inclusions, moment singularities, described by moment intensity factors (MIFs), occur only in cases of sufficiently stiff or sufficiently flexible inclusions.
Keywords: *thin plate, inclusions, cracks, complex potentials, boundary value problem, mathematical modeling, numerical methods, moment intensity factors.*

How to quote: A. Koshkin, and O. Strelnikova, “Bending analysis of multiply-connected anisotropic plates with elastic inclusions”, *Bulletin of V. N. Karazin Kharkiv National University, series Mathematical modelling. Information technology. Automated control systems*, vol. 68, pp. 43-53, 2025. https://doi.org/10.26565/2304-6201-2025-68-04

Як цитувати: Koshkin A., and Strelnikova O. Bending analysis of multiply-connected anisotropic plates with elastic inclusions. *Вісник Харківського національного університету імені В. Н. Каразіна, серія Математичне моделювання. Інформаційні технології. Автоматизовані системи управління*. 2025. вип. 68. С.43-53. https://doi.org/10.26565/2304-6201-2025-68-04

1. Introduction

Despite the significant practical importance of determining the stress state of thin plates under transverse bending, especially in case of presence of foreign inclusions, many engineering problems remain unsolved. It is connected with major mathematical and computational difficulties that have been historically challenging to overcome.

Significant results in developing solution methods for the applied theory of bending of anisotropic plate were obtained by S. G. Lekhnitskii [1] as early as the mid-1930s. Complex potentials were introduced, and the simplest problems for simply-connected domains were solved. Somewhat later, methods for solving problems for multiply-connected plates were developed [2]. However, inaccuracies in the general representations of complex potentials in [2], the use of the series method to satisfy boundary conditions in such complex problems, and the limited computational technology of that time prevented the solution of many relevant problems in plate bending theory. To satisfy the boundary conditions in such complex problems, the discrete least squares method was initially applied, followed by the generalized least squares method (GLSM). This evolution in solution methods allowed to analyse any multiply-connected domains with arbitrarily shaped contours. The GLSM, in particular, proved to be the simplest for computer implementation.

The presence of elastic inclusions in plates introduces additional difficulties in solving these problems. For a plate with elliptical (circular) elastic inclusions under a generalized plane stress state, a large number of problems have been solved [2–4]; plates with linear inclusions have been considered as a special case [5]. In the case of transverse bending of plate, such problems have only been solved for a plate with a single elliptical (circular) inclusion [1, 6] or a single linear inclusion [7]. However, the general case of the bending of a multiply-connected plate with several elastic inclusions, including linear ones, has not been considered.

This article, using the GLSM, presents for the first time a solution to the problem of the bending of an anisotropic plate containing multiple elliptical or linear elastic inclusions. The results of numerous calculations are described, which identify the influence of the elastic inclusions' stiffness, the distances between them, and the geometric characteristics of the inclusions themselves on the bending moment values arising in the plate. Isotropic plates are considered as a special case of anisotropic ones. To simplify the utilized relations, the plate is assumed to be infinite, and the surfaces of the plate and inclusions are unloaded.

2. Problem Formulation and Solution Method

Let us consider an infinite anisotropic plate-matrix, occupying a multiply-connected domain S, bounded by the contours L_l $\left(l=\overline{1,\mathrm{L}}\right)$ of elliptical holes. These holes have semi-axes a_l, b_l, centers at points O_l (with coordinates x_{0l}, y_{0l}), and orientation angles φ_l formed by the x-axis with the semi-axes a_l (Fig. 2.1). Elastic inclusions, occupying domains $S^{(l)}$ and made of different materials, are inserted into these holes without pre-stress. These inclusions are in perfect mechanical contact with the plate. At infinity, the plate is subjected to moments M_x^{∞}, M_y^{∞} and H_{xy}^{∞}.

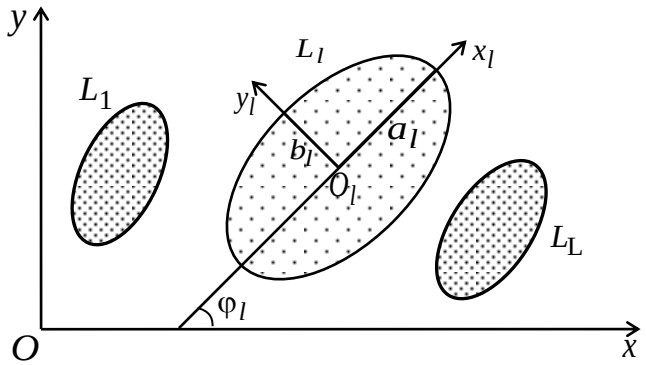

Fig. 2.1 Infinite anisotropic plate with inclusions
Рис. 2.1 Нескінченна анізотропна плита з включеннями

Let’s use the complex potentials from the applied theory of anisotropic plate bending. It leads to finding the complex potentials $W_k'(z_k)$ for the plate-matrix and $W_k'^{(l)}(z_k^{(l)})$ for the inclusions, based on the corresponding boundary conditions.

The complex potentials $W_k'(z_k)$ for the plate-matrix are functions of the generalized complex variables

$$z_k = x + \mu_k y, \tag{2.1}$$

where μ_k are the roots of the characteristic equation

$$D_{22}\mu^4 + 4D_{26}\mu^3 + 2\left(D_{12} + 2D_{66}\right)\mu^2 + 4D_{16}\mu + D_{11} = 0, \tag{2.2}$$

$D_{ij} = B_{ij}D_0$ are the flexural rigidities of the plate material, where

$$B_{11} = (a_{22}a_{66} - a_{26}^2)/\Delta, \quad B_{12} = (a_{16}a_{26} - a_{12}a_{66})/\Delta, \quad B_{16} = (a_{12}a_{26} - a_{16}a_{22})/\Delta$$
$$B_{22} = (a_{11}a_{66} - a_{16}^2)/\Delta, \quad B_{26} = (a_{12}a_{16} - a_{26}a_{11})/\Delta, \quad B_{66} = (a_{11}a_{22} - a_{12}^2)/\Delta,$$
$$\Delta = \begin{vmatrix} a_{11} & a_{12} & a_{16} \\ a_{12} & a_{22} & a_{26} \\ a_{16} & a_{26} & a_{66} \end{vmatrix};$$

a_{ij} are the compliance coefficients of the material; $D_0 = 2h^3/3$; h is the half-thickness of the plate. These functions are defined in the domains S_k, obtained from the original domain S by the affine transformations (2.1), and in our case they can be expressed in next form:

$$W_k'(z_k) = \Gamma_k z_k + \sum_{l=1}^{\mathrm{L}} \sum_{p=1}^{\infty} \frac{a_{klp}}{\zeta_{kl}^p}, \tag{2.3}$$

in which Γ_k are constants determined from the system of equations

$$2\,\mathrm{Re}\sum_{k=1}^{2}\Gamma_k = C_{11}M_x^{\infty} + C_{21}M_y^{\infty} + C_{31}H_{xy}^{\infty},$$
$$2\,\mathrm{Re}\sum_{k=1}^{2}\mu_k\Gamma_k = C_{12}M_x^{\infty} + C_{22}M_y^{\infty} + C_{32}H_{xy}^{\infty},$$
$$2\,\mathrm{Re}\sum_{k=1}^{2}\mu_k^2\Gamma_k = C_{13}M_x^{\infty} + C_{23}M_y^{\infty} + C_{33}H_{xy}^{\infty}, \quad 2\,\mathrm{Re}\sum_{k=1}^{2}\frac{1}{\mu_k}\Gamma_k = 0; \tag{2.4}$$
$$C_{11} = \left(2D_{22}D_{66} - 2D_{26}^2\right)/\Delta_1,$$
$$C_{21} = \left(2D_{16}D_{26} - 2D_{12}D_{66}\right)/\Delta_1,$$
$$C_{31} = \left(2D_{12}D_{26} - 2D_{12}D_{22}\right)/\Delta_1,$$
$$C_{12} = \left(D_{12}D_{26} - D_{16}D_{22}\right)/\Delta_1,$$
$$C_{22} = \left(D_{12}D_{16} - D_{11}D_{26}\right)/\Delta_1,$$
$$C_{32} = \left(D_{11}D_{22} - D_{12}^2\right)/\Delta_1,$$
$$C_{13} = \left(2D_{16}D_{26} - 2D_{12}D_{66}\right)/\Delta_1,$$
$$C_{23} = \left(2D_{11}D_{66} - 2D_{16}^2\right)/\Delta_1,$$
$$C_{33} = \left(2D_{12}D_{16} - 2D_{11}D_{26}\right)/\Delta_1,$$
$$\Delta_1 = \begin{vmatrix} D_{11} & 2D_{16} & D_{12} \\ D_{12} & 2D_{26} & D_{22} \\ D_{16} & 2D_{66} & D_{26} \end{vmatrix};$$

ζ_{kl} are variables obtained from the conformal mappings of the exterior of the unit circle $|\zeta_{kl}| \geq 1$ onto the exterior of the ellipses L_{kl}

$$z_k = z_{kl} + R_{kl}\left(\zeta_{kl} + \frac{m_{kl}}{\zeta_{kl}}\right); \tag{2.5}$$

$$z_{kl} = x_{0l} + \mu_k\, y_{0l},$$
$$R_{kl} = \left[a_l \left(\cos\varphi_l + \mu_k \sin\varphi_l\right) + ib_l \left(\sin\varphi_l - \mu_k \cos\varphi_l\right)\right]/2,$$
$$m_{kl} = \left[a_l \left(\cos\varphi_{_l} + \mu_k \sin\varphi_l\right) - ib_l \left(\sin\varphi_l - \mu_k \cos\varphi_l\right)\right]/2R_{kl}\,; \qquad (2.6)$$

$a_{k\,l\,p}$ are unknown constants.

Once the complex potentials are determined, the plate deflection, bending moments and transverse shear forces are calculated using the formulas [1, 2]:

$$w = 2\,\mathrm{Re}\sum_{k=1}^{2} W_k\left(z_k\right),$$
$$\left(M_x, M_y, H_{xy}, N_x, N_y\right) = -2\,\mathrm{Re}\sum_{k=1}^{2}\left(p_k, q_k, r_k, \mu_k s_k, -s_k\right) W_k''(z_k), \qquad (2.7)$$

in which

$$p_k = D_{11} + 2D_{16}\mu_k + D_{12}\mu_k^2,$$
$$q_k = D_{12} + 2D_{26}\mu_k + D_{22}\mu_k^2,$$
$$r_k = D_{16} + 2D_{66}\mu_k + D_{26}\mu_k^2,$$
$$s_k = -D_{16} - (D_{12} + 2D_{66})\mu_k - 3D_{26}\mu_k^2 - D_{22}\mu_k^3. \qquad (2.8)$$

For the bending moments on elements with a normal n we have:

$$M_n = M_x \cos^2 nx + M_y \cos^2 ny + 2H_{xy} \sin nx \cos nx. \qquad (2.9)$$

The complex potentials $W_k'^{(l)}(\mathrm{z}_k)$ for the inclusions $\left(l = \overline{1,\mathrm{L}}\right)$ are functions of the generalized complex variables

$$z_k^{(l)} = x + \mu_k^{(l)} y, \qquad (2.10)$$

where $\mu_k^{(l)}$ are the roots of characteristic equations of type (2.2), in which the coefficients $D_{i\,j}$ are replaced by the constants $D_{i\,j}^{(l)}$ for the inclusions. These functions are defined in the domains $S_k^{(l)}$ obtained from the domains $S^{(l)}$ by the affine transformations (2.10). They are holomorphic in the domains $S_k^{(l)}$ and can be expanded in series of Faber polynomials, which, after transformations, are represented as power series:

$$W_k'^{(l)}(z_k^{(l)}) = \sum_{p=0}^{\infty} a_{kp}^{(l)} \left(\frac{z_k^{(l)} - z_{kl}^{(l)}}{R_{kl}^{(l)}} \right)^p. \qquad (2.11)$$

Here $R_{kl}^{(l)}$ and $z_{kl}^{(l)}$ are constants calculated by formulas (2.6) for R_{kl} and z_{kl} respectively, substituting μ_k for $\mu_k^{(l)}$; $a_{k\,p}^{(l)}$ are unknown constants.

The unknown constants $a_{k\,l\,p}$ and $a_{k\,p}^{(l)}$ will be determined from the boundary conditions on the contours of the plate and the inclusions:

$$2\,\mathrm{Re}\sum_{k=1}^{2}\left(g_{kli} W_k'(z_k) - g_{kli}^{(l)} W_k'^{(l)}(z_k)\right) = f_{li} \quad (i = \overline{1,4}), \qquad (2.12)$$

in which

$$g_{kl1} = 1, \quad g_{kl1}^{(l)} = 1, \quad g_{kl2} = \mu_k, \quad g_{kl2}^{(l)} = \mu_k^{(l)},$$
$$g_{kl3} = p_k/\mu_k, \quad g_{kl3}^{(l)} = p_k^{(l)}/\mu_k^{(l)}, \quad g_{kl4} = q_k, \quad g_{kl4}^{(l)} = q_k^{(l)};$$
$$f_{l1} = f_{l2} = 0, \quad f_{l3} = -c_l x + c_{1l}, \quad f_{l4} = -c_l y + c_{2l},$$

where c_l are real constants and c_{1l}, c_{2l} are complex constants.

When using the generalized least squares method GLSM, we will satisfy the boundary conditions (2.12) in a differential form in order to eliminate the arbitrary complex constants within them. To do this, we select a set of collocation points $t_{lm} = x_{lm} + iy_{lm}$ $(\mathrm{m} = \overline{1, M_l})$ on the plate-inclusion interface. Then we substitute the functions (2.3) and (2.11) into the boundary conditions (2.12) after differentiating them with respect to the contour arc. This yields a system of linear equations:

$$2\,\mathrm{Re}\sum_{k=1}^{2}\delta_k\left[\sum_{l=1}^{\mathrm{L}}\sum_{p=1}^{\infty} g_{k\,l\,i}\varphi'_{k\,l\,p}\left(t_{km}\right)a_{k\,l\,p} - \sum_{p=1}^{\infty} g^{(l)}_{k\,p}\varphi'^{(l)}_{kp}\left(t^{(l)}_{km}\right)a^{(l)}_{k\,p}\right] =$$

$$= \frac{df_{li}(t_{km})}{ds} - 2\,\mathrm{Re}\sum_{k=1}^{2}\delta_k g_{k\,l\,i}\Gamma_k \quad (l=\overline{1,\mathrm{L}};\ m=\overline{1,M_l};\ i=\overline{1,4}). \tag{2.13}$$

Here,

$$\varphi'_{k\,l\,p} = -\frac{p}{\zeta_{kl}^{p-1}\left(\zeta_{kl}^2 - m_{kl}\right)R_{kl}};\quad \varphi'^{(l)}_{kp} = \frac{p\left(z^{(l)}_k - z_{kl}\right)^{p-1}}{\left(R^{(l)}_k\right)^p};$$

$$\delta_k = dt_k / ds;\quad t_{km} = x_m + \mu_k y_m,\quad t^{(l)}_{km} = x_m + \mu^{(l)}_k y_m.$$

The system (2.13) is supplemented by the single-valuedness conditions for the deflection function $w(x, y)$ for each hole in the plate-matrix

$$2\,\mathrm{Re}\sum_{k=1}^{2} i a_{jkl1}R_{kl} = 0 \quad (l=\overline{1,\mathrm{L}}). \tag{2.14}$$

After finding the pseudo-solutions of the augmented system (2.13) using singular value decomposition (SVD) [8], the constants a_{klp}, $a^{(l)}_{k\,p}$, and consequently, the functions (2.3) and (2.11), become known. The bending moments and shear forces (2.7) can then be determined from them. If an inclusion $S^{(l)}$ is reduced into a linear elastic line (and the corresponding hole into a slit), the moment intensity factors (MIFs) $k_1^{\pm}$ (for moments $M_y^{(l)}$ in the local coordinate system centered at point O_l (see Fig. 2.1)) and $k_2^{\pm}$ (for moments $H_{xy}^{(l)}$ in the same coordinate system) can also be calculated. The superscripts $-$ and $+$ refer to the left and right tips of the inclusion respectively. By analogy with the derivation of stress intensity factors (SIFs) for slit tips in plates [9], the formulas for them are:

$$k_1 = 2\,\mathrm{Re}\sum_{k=1}^{2}\left[p_k\sin^2\varphi_l + q_k\cos^2\varphi_l - r_k\sin 2\varphi_l\right]M_k,$$

$$k_2 = 2\,\mathrm{Re}\sum_{k=1}^{2}\left[\frac{1}{2}\left(q_k - p_k\right)\sin 2\varphi_l + r_k\cos 2\varphi_l\right]M_k, \tag{2.15}$$

It should be noted that in the case of a plate with a single elliptical inclusion, an exact analytical solution can also be obtained using the series method, in the form of:

$$W'_k(z_k) = \Gamma_k z_k + \frac{a_{k11}}{\zeta_{k1}},\quad W'^{(1)}_k(z_k) = a^{(1)}_{k1}\frac{z^{(1)}_k}{R^{(1)}_k},$$

$$\left(M_x, M_y, H_{xy}\right) = -2\,\mathrm{Re}\sum_{k=1}^{2}\left(p_k, q_k, r_k\right)\left(\Gamma_k - \frac{a_{k11}}{R_{k1}\left(\zeta_{k1}^2 - m_{k1}\right)}\right),$$

$$\left(k_1^{\pm}, k_2^{\pm}\right) = \frac{1}{\sqrt{a_1}}2\,\mathrm{Re}\sum_{k=1}^{2}\left(q_k, r_k\right)a_{k11}, \tag{2.16}$$

in which a_{k11} and $a^{(1)}_{k1}$ are constants determined from a system of linear algebraic equations of the 4th order.

3. Numerical studies

Numerical studies were conducted for a plate made of KAST-V isotropic material (Material M1) and angle-ply fiberglass (Material M2). The compliance coefficients for these materials are presented in Table 3.1. In the numerical calculations, the compliance coefficients for the inclusion material were selected as follows: $a_{ij}^{(l)} = \lambda^{(l)} a_{ij}$, where $\lambda^{(l)}$ is the relative stiffness parameter of the inclusion $S^{(l)}$.

Table 3.1. The compliance coefficients of materials
Таблиця 3.1. Коефіцієнти деформації матеріалів

Material	$a_{11}\cdot 10^{-4}, MPa^{-1}$	$a_{22}\cdot 10^{-4}, MPa^{-1}$	$a_{12}\cdot 10^{-4}, MPa^{-1}$	$a_{66}\cdot 10^{-4}, MPa^{-1}$
M1	72,100	72,100	-8,600	161,500
M2	10000	2,800	-0,770	27,000

During the numerical studies, the number of terms N in the series functions (2.3) and (2.11) and the number of collocation points M_l on the plate-inclusion interface (where conditions (2.13) were satisfied) were increased until the boundary conditions were met with a sufficiently high degree of accuracy. The calculations showed that, depending on the distances between inclusions and the semi-axis ratios of the ellipses, satisfying the boundary conditions required retaining from 7 to 20 terms in the series for each hole and inclusion, and selecting from 50 to 1000 collocation points on each contour. Below, some of the obtained results are described for the case where, at infinity, $M_y^{\infty} = m_y$ and $M_x^{\infty} = H_{xy}^{\infty} = 0$. All results are presented as multiples of m_y / D_0. For the case of a plate with a single inclusion, the exact solution (2.16) was also used for comparison.

It was established that the moment values are significantly influenced by the semi-axis ratio of the ellipses. Calculations showed that for $b_1/a_1 < 10^{-3}$ the inclusion can be considered linear, and MIFs (Moment Intensity Factors) can be calculated for it. In Table 3.2, the M_s moment values for a plate with a single inclusion are presented. These values are shown for points on the plate near the inclusion and for various semi-axis ratios b_1/a_1 and relative stiffness parameters $\lambda^{(1)}$. For the case of a linear inclusion ($b_1/a_1 = 10^{-4}$), the MIFs are also presented.

Table 3.2. The M_s moment values for a plate with a single inclusion
Таблиця 3.2. Значення моментів M_s для плити з одним включенням

Material	$\lambda^{(1)}$	b_1/a_1						MIF
		1	0,5	10^{-1}	10^{-2}	10^{-3}	10^{-4}	$k_1^{\pm}$
M1	0	-0,16	-0,19	-0,42	-3,02	-29,00	-288,69	-0,136
	10^{-2}	-0,12	-0,16	-0,33	-0,97	-1,32	-1,38	-0,001
	0,5	0,72	0,63	0,53	0,50	0,49	0,49	0,000
	2	1,25	1,40	1,77	1,97	1,99	1,99	0,000
	10^2	1,70	2,40	7,62	42,10	86,81	97,28	0,013
	∞	1,72	2,44	8,18	72,78	718,83	7178,87	1,000
M2	0	-0,22	-0,27	-0,69	-5,37	-52,18	-520,13	-0,170
	10^{-2}	-0,19	-0,24	-0,53	-1,51	-1,99	-2,06	-0,001
	0,5	0,65	0,58	0,51	0,49	0,49	0,49	0,000
	2	1,37	1,55	1,86	1,97	1,99	1,99	0,000
	10^2	2,31	3,59	12,71	57,10	91,35	97,22	0,007
	∞	2,35	3,70	14,48	135,77	1348,63	13475,67	1,000

It is evident that as the ratio b_1/a_1 decreases, the absolute values of the moments M_s near the tips of the major semi-axis a_1 increase sharply, and for small b_1/a_1 values, this indicates the singular behavior characterized by MIFs.

Fig. 3.1 shows plots of the MIF ($k_1^{\pm}$) variation as a function of the inclusion material stiffness (parameter $\lambda^{(1)}$). It can be seen that for a linear inclusion, when $\lambda^{(1)} < 10^{-3}$, the inclusion can be considered perfectly rigid; when $\lambda^{(1)} > 10^3$, it is considered perfectly flexible (a crack). For $10^{-3} < \lambda^{(1)} < 10^3$ the MIF values are very small and can be neglected. Therefore, it is not meaningful to discuss MIFs for linear elastic inclusions when their material stiffness differs from that of the plate material by less than a factor of 10^3, although other authors, using different models and methods, have reached different conclusions [7]. It should also be noted that for perfectly flexible linear inclusions (cracks), their faces will come into contact. This must be accounted for when solving such problems, for instance, by applying appropriate additional tensile forces. These issues are not addressed in this study. We note that the exact solution (2.16) was also used for the plate with a single inclusion. The results obtained from the approximate GLSM solution were found to coincide with the results from the exact solution.

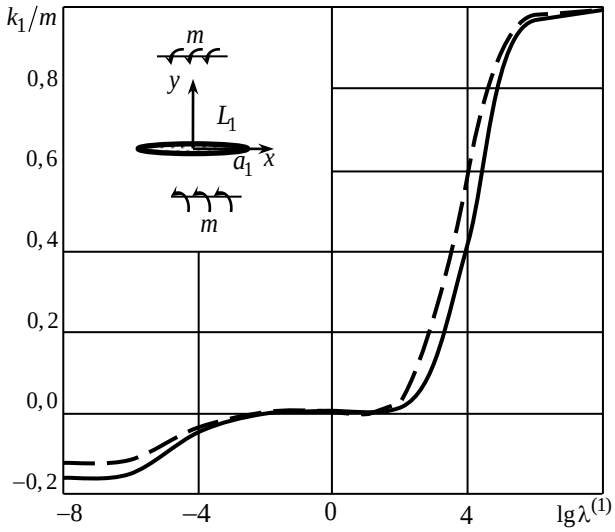

Fig. 3.1 MIF variation depending on inclusion stiffness
Рис. 3.1 Зміна КІМ в залежності від жорсткості включення

Table 3.3 presents the bending moment values M_s for an infinite plate with two identical circular inclusions (Fig. 3.2) of radius a_1 $(b_1 = a_2 = b_2 = a_1)$. The values are given for various distances c between the inclusions and various values of the relative stiffness parameter $\lambda^{(1)}$ (where $\lambda^{(2)} = \lambda^{(1)}$). The moments are calculated at the contact points of the plate with the left inclusion, on elements perpendicular to the inclusion contour. Here, θ is the central angle for the left inclusion, measured counter-clockwise from the line of centers.

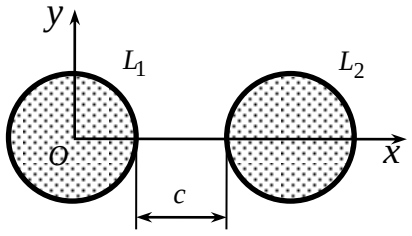

Fig. 3.2 Infinite anisotropic plate with two circular inclusions
Рис. 3.2 Нескінченна анізотропна плита з двома круговими включеннями

The data in Table 3.3 show that as the distance between the inclusions decreases, the M_s moment values at points near the ligament (the area between the inclusions) increase. If the distance between the inclusions is greater than the diameter of one of them ($c/a_1 > 2$), the influence of one inclusion on the stress state around the other is insignificant and can be neglected. As the stiffness of the inclusions decreases (with an increase of $\lambda^{(1)}$), the M_s moment values at the point corresponding to $\theta = 0$ (at the ligament) increase. At the point corresponding to $\theta = \pi/2$, the moments decrease for $\lambda^{(1)} > 1$ (i.e., stiffer inclusions) and increase for $\lambda^{(1)} < 1$ (i.e., more flexible inclusions).

Table 3.3. The M_s moment values for a plate with two inclusions
Таблиця 3.3. Значення моментів M_s для плити з двома включеннями

$\lambda^{(1)}$	c/a_1	θ, *rad*					
		0	$\pi/2$	π	0	$\pi/2$	π
		M1			M2		
0	∞	-0,16429	0,37740	-0,16429	-0,22231	0,19019	-0,22231
	2	-0,15829	0,31479	-0,08789	-0,24754	0,17038	-0,14703
	1	-0,12078	0,26235	-0,01533	-0,26818	0,15308	-0,04814
	0.5	-0,04908	0,21283	0,03215	-0,28425	0,13658	0,05675
	0.1	0,12031	0,18256	0,00779	-0,43370	0,12183	0,10487
10^{-2}	∞	-0,12351	0,35057	-0,12351	-0,18512	0,17639	-0,18512
	2	-0,12717	0,29375	-0,05347	-0,21340	0,15806	-0,11195
	1	-0,07491	0,24712	0,01489	0,22438	0,09538	0,33411
	0.5	-0,15650	0,18608	0,04670	0,22850	0,05939	0,55252
	0.1	-0,13326	0,17431	0,14177	0,41496	0,11151	0,74618
0,5	∞	0,71970	-0,00208	0,71970	0,65308	-0,00633	0,65308
	1	0,61813	-0,00630	0,72212	0,58172	-0,00825	0,66258
	0.1	0,53298	-0,01874	0,74171	0,39733	-0,01669	0,72451
2	∞	1,24827	0,05753	1,24827	1,36933	0,04577	1,36933
	1	1,39080	0,05634	1,26801	1,47429	0,04405	1,38645
	0.1	1,70994	0,06741	1,26061	1,89385	0,05277	1,35439
10^2	∞	1,70384	0,27407	1,70384	2,31079	0,25327	2,31079
	2	1,92563	0,26062	1,77606	2,48063	0,24013	2,38868
	1	2,24528	0,26094	1,82188	2,76070	0,23748	2,45147
	0.5	2,80183	0,26642	1,86998	3,38583	0,23875	2,52330
	0.1	4,23279	0,29051	1,93290	2,54783	0,18390	1,99577
∞	∞	1,71784	0,28251	1,71784	2,34765	0,26278	2,34765
	2	1,94561	0,26859	1,79201	2,52289	0,24917	2,42875
	1	2,27663	0,26857	1,83915	2,81262	0,24625	2,49507
	0.5	2,86793	0,27381	1,88746	3,45585	0,24880	2,57465
	0.1	5,62046	0,28538	1,97168	7,32184	0,26064	2,74416

Numerical studies were also conducted for the case of two linear inclusions. Fig. 3.3 shows the variation of the MIF ratio k_1^+ / k_{10}^+ for the isotropic material M1, where k_1^+ represents the MIF at the inner tip (right tip of the left inclusion) and k_{10}^+ is the baseline MIF for an isolated single inclusion. For material M2, the corresponding graph differs only slightly from that shown in Fig. 3.3, and therefore it is not depicted. It is evident that as the distance between the linear inclusions decreases, the MIFs for the inclusions' inner tips increase significantly.

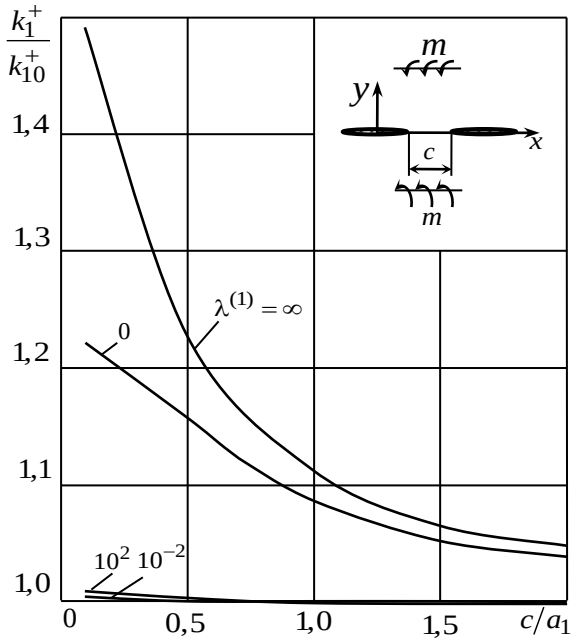

Fig. 3.3 Variation of the MIF ratio for case of two linear inclusions
Рис. 3.3 Зміна відношення КІМ для випадку двох лінійних включень

4. Conclusions

In this paper, a new effective approximate method for analyzing the stress state of thin anisotropic plates with multiple elastic inclusions under bending has been developed. The approach is based on the application of complex potentials, their representation by Laurent series and Faber polynomials, and the implementation of the Generalized Least Squares Method to satisfy the contact boundary conditions. The problem is reduced to solving an overdetermined system of linear algebraic equations using Singular Value Decomposition (SVD).

The high accuracy and reliability of the proposed method were validated by comparing its results with the known exact analytical solution for the case of a single elliptical inclusion, demonstrating perfect agreement.

The primary scientific contributions of this work are:

1. A robust computational framework capable of handling multiple, arbitrarily oriented elliptical or linear inclusions, a problem not previously solved in the general case.
2. A key finding regarding linear inclusions: it was established that moment singularities, described by MIFs, arise only for sufficiently stiff ($\lambda^{(1)} < 10^{-3}$) or sufficiently flexible ($\lambda^{(1)} > 10^{3}$) inclusions.
3. The significant effect of inclusion interaction was quantified. For both circular and linear inclusions, it was shown that as the distance between them decreases, the stress (moment) concentration in the ligament region increases substantially.

The developed method demonstrates significant potential for further development. Future research could focus on several promising directions:

- Analyzing periodic or finite arrays (rows and bands) of inclusions to effectively model the mechanical behavior of modern composite structures.
- Extending the method to analyze inclusions of arbitrary (non-elliptical) shapes, which are common in engineering practice, by employing advanced conformal mapping techniques and polynomial approximations.

REFERENCES

1. S.G. Lekhnitskii, S.W. Tsai and T. Cheron, *Anisotropic Plates*. New York: Gordon and Breach, 1968, 534 p. https://books.google.com.ua/books?id=Ukl9AAAAIAAJ
2. G.N. Savin, *Stress distribution around holes*. Washington, D.C.: NASA TT, 1970, 997 p. https://books.google.com.ua/books?id=eC9e0QEACAAJ

3. C. Hwu and J. Yen Wen, “On the Anisotropic Elastic Inclusions in Plane Elastostatics”. *J. Appl Mech*, vol. 60 (3), pp. 626–632, 1993. https://doi.org/10.1115/1.2900850
4. C. Hwu, *Anisotropic Elastic Plates*. New York: Springer, 2010, 673 p. https://doi.org/10.1007/978-1-4419-5915-7
5. J. Lee, “Elastic analysis of unbounded solids using volume integral equation method”. *J Mech Sci Technol*, vol. 22, pp. 450–459, 2008. https://doi.org/10.1007/s12206-007-1215-2
6. M.C. Hsieh and C. Hwu, “Anisotropic elastic plates with holes / cracks / inclusions subjected to out-of-plane bending moments”. *Int. J. Solids and Struct*, vol. 39, no. 19, pp. 4905–4925, 2002. https://doi.org/10.1016/S0020-7683(02)00335-9
7. O.V. Maksymovych, T.Y. Solyar and Y. Kempa, “Investigation of Bending of Anisotropic Plates with Inclusions with the Help of Singular Integral Equations”. *J Math Sci*, vol. 254, pp. 129–141, 2021. https://doi.org/10.1007/s10958-021-05293-7
8. Z. Drmač and K. Veselić, “New fast and accurate Jacobi SVD algorithm. I”. *SIAM J. Matrix Anal. Appl*, vol. 29, no. 4, pp. 1322–1342, 2008. https://doi.org/10.1137/050639193
9. G.C. Sih, P.C. Paris and G.R. Irwin, “On cracks in rectilinearly anisotropic bodies”. *Int J Fract*, vol. 1, pp. 189–203, 1965. https://doi.org/10.1007/BF00186854

Кошкін Андрій Олександрович *асистент кафедри прикладної математики*
Харківський національний університет радіоелектроніки, пр. Науки, 14, м. Харків, 61166, Україна

Стрельнікова Олена Олександрівна *д.т.н., проф. кафедри прикладної математики*
Харківський національний університет радіоелектроніки, пр. Науки, 14, м. Харків, 61166, Україна
провідний науковий співробітник
Інститут енергетичних машин і систем ім. А. М. Підгорного НАН України, вул. Комунальників, 2/10, м. Харків, 61023, Україна

Аналіз згину багатозв’язних анізотропних плит з пружними включеннями

Актуальність. Визначення напружено-деформованого стану тонких анізотропних плит з інородними пружними включеннями при поперечному згині є важливою інженерною задачею. Однак загальний випадок плити з декількома довільно розташованими включеннями досі не мав ефективного чисельного або аналітичного розв'язку через значні математичні та обчислювальні труднощі.
Мета. Метою роботи є розробка нового наближеного методу для визначення напруженого стану тонкої анізотропної плити, що містить групу довільно розташованих еліптичних або лінійних пружних включень.
Методи дослідження. Метод базується на застосуванні комплексних потенціалів С. Г. Лехницького. Задача зводиться до визначення функцій узагальнених комплексних змінних для плити-матриці та включень. Ці потенціали представляються відповідними рядами Лорана та поліномами Фабера. Для задоволення контактних граничних умов на контурах включень використовується узагальнений метод найменших квадратів (УМНК). Це зводить задачу до перевизначеної системи лінійних алгебраїчних рівнянь, яка розв'язується за допомогою сингулярного розкладу (SVD).
Результати. Розроблений метод було перевірено шляхом порівняння з відомим точним аналітичним розв'язком для плити з одним еліптичним включенням, що показало повний збіг результатів. Проведено чисельні дослідження впливу відносної жорсткості включень, відстаней між ними та їхніх геометричних характеристик на значення згинальних моментів. Встановлено, що взаємодія між включеннями є суттєвою та призводить до значного зростання моментів при малих відстанях між ними. Ізотропні плити розглядались як окремий випадок анізотропних.
Висновки. Вперше встановлено, що для лінійних пружних включень особливості моментів, які описуються коефіцієнтами інтенсивності моментів (КІМ), виникають лише у випадках достатньо жорстких або достатньо гнучких включень.

Ключові слова: *тонка плита, включення, тріщини, комплексні потенціали, крайова задача, математичне моделювання, чисельні методи, коефіцієнти інтенсивності моментів.*

Надійшла у першій редакції 07.10.2025; в останній 11.11.2025; опубліковано 30.12.2025.
The first version has been received on 07.10.2025; the final version on 11.11.2025; published 30.12.2025.